ANNALS of Faculty Engineering Hunedoara
– International Journal of Engineering
Tome XIII [2015] – Fascicule 4 [November]
ISSN: 1584-2673 [CD-Rom; online]
a free-access multidisciplinary publication of the Faculty of Engineering Hunedoara

[1.] Andrei CRISAN

EXPERIMENTAL AND NUMERICAL DETERMINATION OF AXIAL STRENGTH FOR PALLET RACKS UPRIGHTS

[1.] University Politehnica Timisoara, Department of Steel Structures and Structural Mechanics, ROMANIA

Abstract: Present paper presents the experimental and numerical approach for determining the axial strength of cold formed pallet rack uprights sections with and without perforations in accordance to European design code. The study presented hereafter is part of an extended experimental and numerical study carried out within the CEMSIG Research Centre (http://cemsig.ct.upt.ro), dep. of Steel Structures and Structural mechanics, POLITEHNICA University of Timisoara. Furthermore, as observed by many researchers, the influence of end restraints, particularly warping, is of paramount importance when discussing about distortional buckling. Using calibrated and validate finite element models, a numerical study was conducted to determine the influence of end restraints, warping in particular, on perforated and unperforated pallet rack uprights sensitive to distortional buckling. The simulations have been conducted on a pallet rack upright section sensitive to distortional buckling, considering short (distortional buckling length range) and long specimens (interactive distortional – global buckling range).
Keywords: Pallet rack uprights, experimental tests, numerical analysis, buckling analysis, warping

1. INTRODUCTION

Racking systems are load bearing structures for the storage and retrieval of goods in warehouses. The goods to be stored are generally on pallets or in box-containers. Racking is constructed from steel components including upright frames, beams and decking. Special beam to column (upright) connections and bracing systems are utilised, in order to achieve a three dimensional steel 'sway' or 'braced' structure with "aisles" to enable order pickers, industrial trucks or stacker cranes to reach the storage positions. Although components are standardised, they are only standard to each manufacturer. These components differ from traditional column and beam structures in the following regard: i) continuous perforated columns (uprights), ii) hook-in connections and iii) structural components for racking generally consist of cold formed thin gauge members.

Because of the differences in shape of structural components, detailing and connection types, additional technical information to the Eurocodes are required. The European Standard, EN15512:2009 [1] specifies the structural design requirements applicable to all types of adjustable beam pallet rack systems fabricated from steel members, intended for the storage of unit loads and subject to predominantly static loads. It gives guidelines for the design of clad rack buildings where requirements are not covered in EN1993 [2]. Pallet racks are standard products for which design by calculation alone aren't enough to characterize the behaviour and capacity of structural members. Test procedures are therefore specified where current analytical methods are not given, or are not appropriate.

Despite their lightness pallet rack systems are able to carry very high loads and also raise considerable height. Usually, uprights members are of mono-symmetrical sections, subjected to axial compression and bending about both axes. The slenderness of cold-formed sections imposes to consider three buckling modes, i.e.: local, distortional and global; often, at least two of these modes might couple. Therefore, such structures, characterised by a complex structural behaviour, have to be carefully designed, and because of lack of adequate analytical models in current design codes, on this purpose test based procedures are used.

The forerunners of the modern storage structures were slotted-angle products first introduced in the 1930s. These consisted of cold-formed angle sections with perforations to provide a means whereby the designer could utilize the simplicity and flexibility of connections thus permitted to produce storage systems in a variety of shapes and configurations. These simple profiles were the starting point for today's upright sections. In the beginning, the upright sections were a perforated C type profile because of the ease of production. In order to raise the buckling strength of the webs, small groove stiffeners were folded in. This eliminated the local buckling problem, but created what Thomasson [3] called a "local-torsional" problem – i.e. distortional buckling. Therefore, optimization of the shape of sections on the purpose to avoid the local buckling creates condition for distortional modes.

Analytical and numerical based methods have been proposed to evaluate the distortional strength of thin-walled cold-formed steel sections [4] - [7]. Even if in the last years numerous investigations were devoted to the effects of holes and member slenderness on the ultimate capacity of pallet rack uprights, no analytical method for the design of rack structures is generally accepted. For this reason, the design of these structures is based on experimental tests prescribed by specific codes. Recent, Moen & Schafer [8] reported the tentative to use of Direct Strength Method for perforated thin-walled sections, but, at the end, concluding is still not possible to avoid testing in design of storage rack structures. The European Standard EN15512:2009 [1] provide experimental procedures for compression tests on stub columns for local buckling, upright members, for distortional buckling, and upright frame units for overall buckling and interaction with local modes.

2. EXPERIMENTAL PROGRAM

The experimental program is part of an extended study devoted to interactive buckling of compression members of steel pallet racks, carried out at the CEMSIG Research Centre (http://cemsig.ct.upt.ro) of "Politehnica" University of Timisoara [9].

2.1. Geometry, material and imperfections

There were tested two heavy-duty rack upright's sections. The cross sections have extended rear flanges (lipped) with nominal dimensions (provided by the manufacturer) presented in Figure 1. The studied sections have the same general geometry. The perforation layout consists in staggered perforations with a pitch (the spacing of the centres of two consecutive holes in the chain measured parallel to the member axis) of 25mm (see Figure 1, side view) and the distance between two identical perforations of 50mm (see Figure 1, back view).

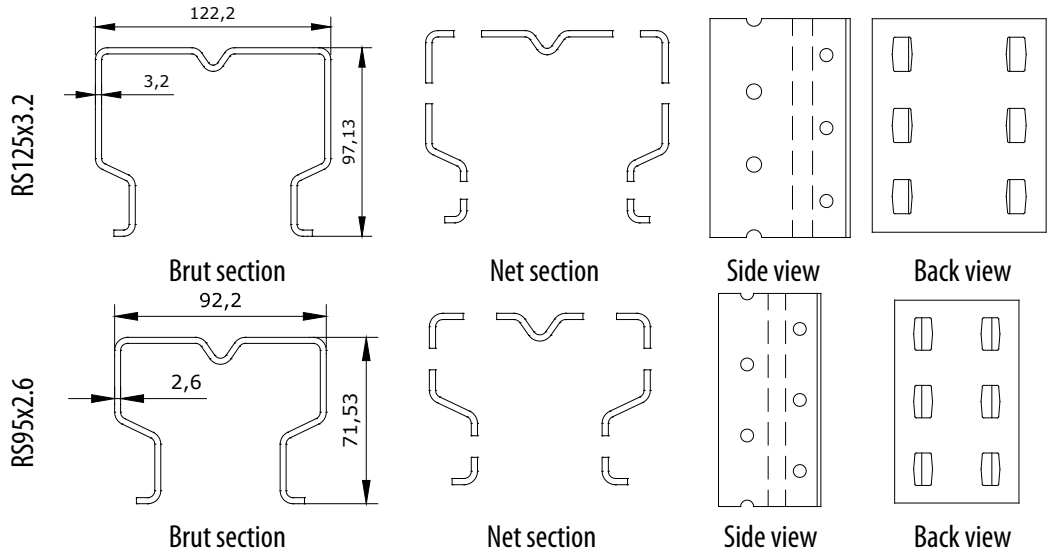

Figure 1. Specimen cross-section – brut (RSB) and perforated (RSN)

Material properties play an important role in the performance of thin walled structural members. For pallet rack uprights, the usual material is steel. It is important to determine the mechanical properties of the steel sheets used in cold-formed steel construction before designing this type of steel structural members.

In order to experimentally determine the mechanical properties, a set of samples were cut out from the base material. The shape and dimensions of testing samples were in accordance with EN10002-1 [10] provisions, function of material thickness. There were tested a total number of ten samples, five for each type of base material. A computer controlled INSTRON 1000KN Dynamic Testing System equipped with an optical extensometer was used to determine the main mechanical characteristic and establish the behaviour curves (stress-strain diagram) for the of base material together with relevant material properties (e.g. yield strength, ultimate strength).

Since the material in the corners of a section is cold-worked to a considerably higher degree than the material in the flat areas, the mechanical properties are different in various parts of the cross section. In order to experimentally determine the yield strength and ultimate tensile strength increase over the cross-section a new series of determinations on coupons cut from specimens without perforations was done for the both of studied sections. For this, three cold formed profiles were cut into strips as show in Figure 2.

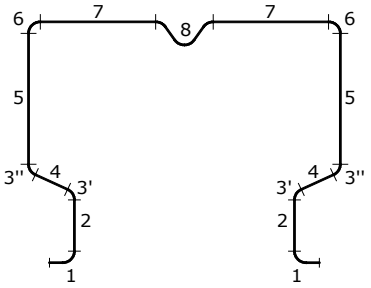

Figure 2. Section strip partition

Further, Figure 3 and Figure 4 present the behaviour curves for RS95x2.6 and RS125x3.2 sections, for the base material a) and for the cold formed sections b).

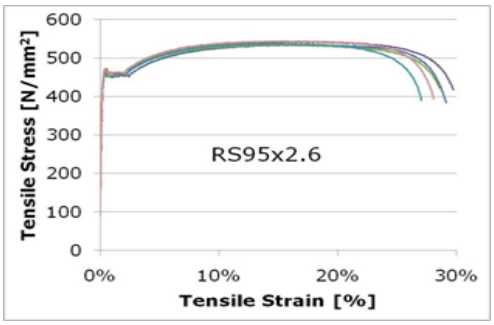

a) base material b) cold formed section

Figure 3. Behaviour curves for a) base material and b) cold formed RS95x2.6 section

a) base material b) cold formed section

Figure 4. Behaviour curves for a) base material and b) cold formed RS125x3.2 section

Comparing the presented behaviour curves, it can be observed that the yield and ultimate strength increase is not uniform over the cross section. For flat areas, the yield strength increase is limited (about 4%). For corner areas, where the cold working is significant, the yield strength increase is higher (more than 25% in some cases).

In the same time, the ductility is reduced down to less than 5%, in some cases. The decrease in ductility is more severe in the case of RS125 section and it can be observed for flat areas as well. This reduction is not necessary a problem for thin walled sections, since an elastic design is usually implied for of cold formed sections.

Before testing, all tested specimens were measured in order to determine the geometric imperfections. Two types of imperfections were recorded, i.e. (a) sectional and (b) global, as presented in Figure 5. For stub columns, the sectional imperfections were measured in 3 sections.

a) b)

Figure 5. Measured imperfections: a) sectional and b) global

Figure 6. Set up for measuring imperfections of upright specimens

For upright sections, the geometric deviations were measured in five equidistant sections along the length. The specimen was mounted between the headstock and the tailstock of a lathe, together with its end assembly (end plates, pressure pads and ball bearings)(see Figure 6). After a measurement was done, the specimen was rotated in order to permit another measurement. The overall imperfections have been measured in the same sections along the specimen's length as the sectional deviations. These values are relative to the upright end, considered as reference.

2.2. STUB column test

According to European standard EN15512:2009 [1], the purpose of stub column testing is to observe the influence of such factors as perforations and local buckling on the compressive strength of a short column. The test setup and the testing procedure are detailed in Annex A.2.1.2 (Alternative 1) of EN15512:2009 [1] design code and summarized hereafter. The length of specimens was determinate with respect to the code requirements i.e.:

i) the length of specimen shall be three times the greatest flat width of the section (ignoring intermediate stiffeners) and it shall include at least five pitches of the perforations;
ii) the test specimen shall be cut normal to longitudinal axis, midway between two sets of perforations;
iii) the base and cap plates shall be bolted or welded to each end of the stub upright.

The section may be adjusted for spring back (distortion of the shape of the cross-section after the cutting due to residual stresses) by welding to the base plates. This test shall not be used to observe the influence of distortional buckling, since it is known that the wavelength for distortional buckling is longer than that for local buckling. This means that distortional buckling is not usually identified by a conventional stub-column test. Furthermore, if a stub-column test exhibits a distortional failure mode, it is unlikely that the length is sufficient to determine the minimum distortional buckling load.

Based on the above mentioned criteria, the length of stub upright presented in Table 1, where f_w is the greatest flat width of the section, ignoring the intermediate stiffeners, *c* is the length of the cold formed section, *a* is the base/cap plate thickness, *p* is the pressure pad thickness (not considering the ball indentation of 5mm), *b* is the buckling length, which includes the length of the cold formed section, base/cap plates, pressure pads (including the ball indentations -5mm x 2) and the ball bearings (2 x 40mm/2).

Table 1. STUB test specimen lengths

Section	f_w [mm]	c [mm]	a [mm]	p [mm]	b [mm]
RS125x3.2	125	400	10	30	510
RS95x2.6	95	300	10	30	410

The test setup is presented in detail in Figure 7 (*a* is base/cap plate, *b* is buckling length of the specimen and c is the length of the cold formed stub upright).

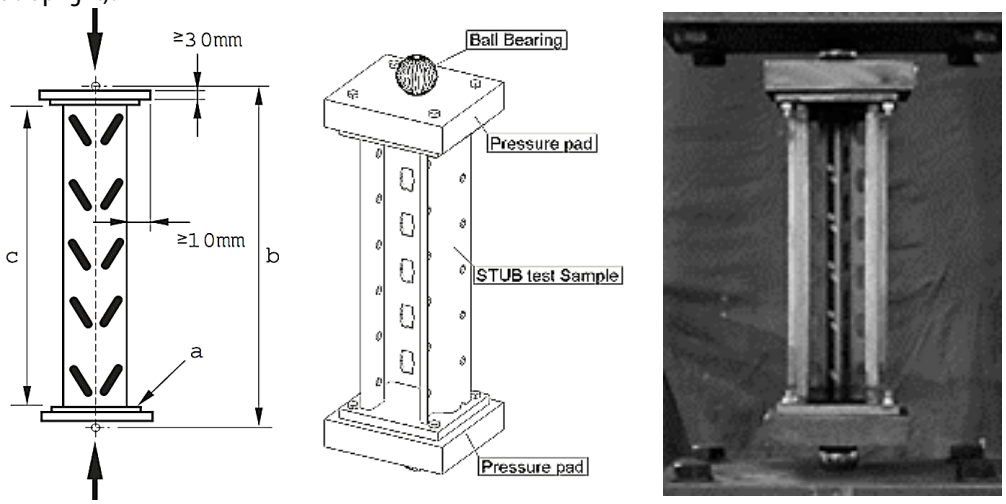

a) EN15512:2009 [1] b) schematic setup c) real setup

Figure 7. Stub column test setup

The European standard does not require tests on specimens without perforations. Even so, tests on specimens without perforations were performed within the framework of this study, in order to quantify the influence of perforations on the capable force of the cross-section. In Table 2 are presented the failure loads for RS95x2.6 and RS125x3.2 stub column specimens, sections with and without perforations.

For RS95x2.6 specimens, the failure mode can be qualified as sections squashing.

The observed failure mode for RS125x3.2 specimens can be categorized as a sections' distortion. Even if the failure mode is similar to a distortional buckling failure mode, the length of STUB column test samples is not enough to determine the critical (minimum) distortional buckling load.

Taking into consideration the results of stub column tests, presented in detail in [11], it can be concluded that none of the tested sections, RS95x2.6 and RS125x3.2, with and without perforations, are prone to local buckling.

In order to quantify the effects of perforations and sectional buckling, an effective area was determined based on stub column tests. The results are presented in Table 3. The effective area presented in Table 3 is informative. The procedure defined by EN15512:2009 [1] takes into account the nominal yield strength, the observed yield strength and the thickness variation together with the standard deviation. Since this is not the main objective, the procedure will not be further detailed.

Analysing the results presented in Table 3, it can be easily observed that for RS125x3.2 brut section, the influence of sectional buckling is relatively high (16%). Furthermore, the perforations decrease the sectional capacity further (28%). For the RS95x2.6 brut section, the plastic capacity anticipated during tests (failure due to squashing) can be observed in Table 3. No reduction due to sectional buckling occurred for this section. On the other hand, the capacity reduction due to perforations is higher than for RS125x3.2 section (20%).

Table 2. Failure loads stub column specimens

Test type	RS95Brut	RS95Net	RS125Brut	RS125Net
Buckling length	410 mm	410 mm	510 mm	510 mm
Samples tested	6	12	6	12
Experimental failure load [kN]	350.68 346.44 346.23 346.63 354.30 338.88	279.82 276.99 284.28 274.33 278.78 278.63 281.63 278.68 279.00 277.92 277.81 283.42	453.90 479.43 463.69 449.52 485.38 487.05	413.28 407.81 400.85 404.03 402.27 400.19 397.46 409.05 411.02 396.51 395.91 406.05
Failure mode (example)	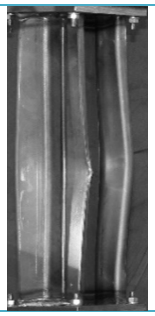	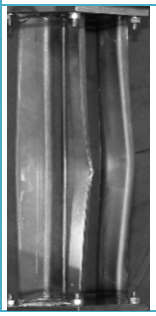		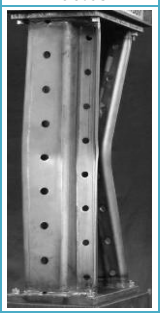

Table 3. Effective areas and equivalent thickness for STUB column specimens

Section	Average test load [kN]	f_{ya} [2] [N/mm^2]	Brut area [mm^2]	Effective area [mm^2]	Reduction %
RS125Brut	469.83	501.29	1111	937	16%
RS125Nnet	403.70			805	28%
RS95Brut	347.19	500.15	694	694	0%
RS95Net	279.27			558	20%

2.3. UPRIGHT column test

The EN15512:2009 [1] design code (section 9.7.2, alternative c) states that the influence of distortional buckling mode on the axial load capacity of the upright section shall be determined by tests. On this purpose, another series of experimental tests have been conducted to evaluate this effect. The obtained results provide a means of correcting the theoretically obtained axial capacity which can be calculated in accordance with section 9.7.4 and 9.7.5 of the same standard. The length of the testing specimens, as specified in section 9.7.2 paragraph c), should be the length of a single bracing panel closest to one metre. For tested sections, the length of the bracing panels was 1200mm, which was considered to be the buckling length of the upright specimens (including base plates, pressure pads and the ball bearings).

The experimental setup was the same as for stub column testing (see Figure 7). In Table 4 are presented the failure loads for RS95x2.6 and RS125x3.2 upright column specimens, sections with and without perforations.

Table 4. Failure loads and failure mode for RS125x3.2 stub column specimens

Test type	RS95Brut	RS95Net	RS125Brut	RS125Net
Buckling length	1200 mm	1200 mm	1200 mm	1200 mm
Samples tested	5	10	5	10
Experimental failure load [kN]	270.35 270.49 272.06 279.65 269.83	207.18 215.72 209.87 211.29 206.45 213.24 223.33 216.30 208.90 209.91	386.72 369.12 386.90 373.41 382.59	347.26 363.48 350.79 339.09 344.46 337.18 354.40 350.45 340.54 345.41
Failure mode (example)				

Initially, at the maximum load the RS95x2.6 upright specimens, section without perforations initiate a distortional failure; the failure mode changed suddenly, jumping to a flexural or flexural-torsional buckling failure mode. The same failure mechanism was observed for RS95x2.6 upright specimens, section with perforations. For RS125x3.2 sections with and without perforations, the failure mode is similar to distortional buckling. Arguably, due to specimens' length, the test results correspond rather to the distortional–global interaction, than to pure distortion.

3. NUMERICAL SIMULATIONS

3.1. Model calibration and validation

The numerical models applied to simulate the behaviour of pallet rack upright members, have been created using the commercial FE program, ABAQUS/CAE v.6.7 [12]. The numerical models were calibrated to replicate the experimental tests. Rectangular 4-noded shell elements with reduced integration (S4R) were used to model the thin-walled cold-formed members. The material behaviour used for numerical modelling was in accordance with the recorded curves from tensile tests from coupons cut over the cross-section (see Figure 3 and Figure 4).

The base plates and pressure pads were modelled using RIGID BODY with PINNED nodes constraints. The reference point for the constraints was considered the centre of the ball bearings (55mm outside the profile), in the gravity centre of the cross-section (see Figure 8).

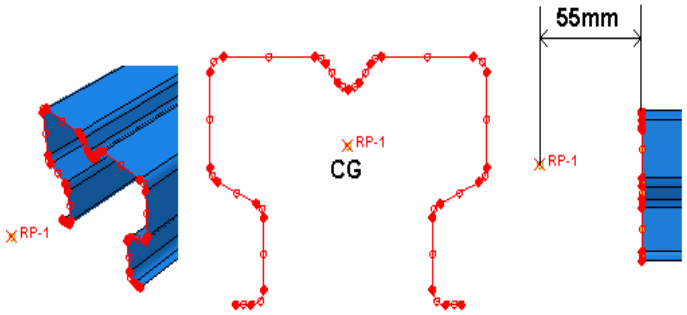

Figure 8. FE model end constraints

For numerical simulations, the specimens were considered pinned at one end and simply supported at the other one. For the pinned end, all three translations together with the rotation along the longitudinal axis of the profile were restrained, while the rotations about maximum and minimum inertia axes were allowed. For the simply supported end, the translations along section axis and the rotation about longitudinal profiles axis were restrained, while the rotations about major and minor inertia axis together with longitudinal translation were allowed.

The analysis was conducted in two steps.

i) The first step consists into a linear buckling analysis (LBA), in order to find a buckling mode or combination of buckling modes, affine with the relevant measured imperfections.

ii) After imposing the initial geometric imperfection, obtained as a linear combination of eigen buckling modes obtained in the previous step, a Geometrically and Materially Nonlinear with Imperfections Analysis (GMNIA) with arc-length solver (static, Riks) was used to determine the profiles' capacity.

A unit displacement was applied at the simply supported end, incremented during the analysis, in order to simulate a displacement controlled experimental test.

Table 5. Numerical and experimental ultimate load for RS125x3.2 stub column

RSB125x3.2	FE model	Experimental tests
Observed failure mode	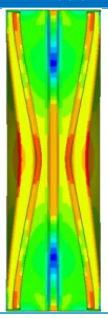	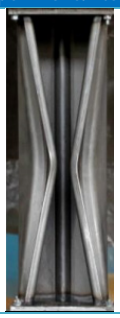
Ultimate load [kN]	461.7	453.90
Difference [%]	+1.72	

In Table 5 are shown, comparatively, the failure modes and the results obtained numerically for RSB125x3.2 section, with and without considering the residual stresses and the experimental test results.

The calibrated numerical model was validated against experimental tests for all tested profiles sets. In Table 6 presents the values of ultimate load from numerical simulations and the experimental ones for all types of members (stub and upright), for both RS125x3.2 and RS95x2.6 cross-sections, with and without perforations.

Table 6. Ultimate load [kN] – Experimental vs. FEM

RSBs125×3.2		RSNs125×3.2		RSBs95×2.6		RSNs95×2.6	
EXP	FEM	EXP	FEM	EXP	FEM	EXP	FEM
487.05	486.13	411.02	422.98	338.88	335.15	274.33	272.01
RSBu125×3.2		RSNu125×3.2		RSBu95×2.6		RSNu95×2.6	
EXP	FEM	EXP	FEM	EXP	FEM	EXP	FEM
386.72	384.40	347.26	344.00	279.65	285.96	223.33	231.89
(s) Stub columns; (u) Upright member specimens; N/B – perforated/brut							

Based on the results obtained from numerical simulations (see Table 6), it can be noted that from the point of view of maximum load, the numerical model is able to accurately replicate the experimental tests. For specimens with increased length, where global

and sectional imperfections are of same importance, a more complex imperfections measurement is recommended. The measurements should allow the decomposition of geometric imperfections into sectional and global components that can afterwards be used to reconstruct the initial deformed shape.

The decomposition method used in this case is limited to symmetric sectional buckling mode and/or global buckling. Further development and more complex measuring are required in order to replicate all experimentally obtained failure modes.

3.2. Numerical simulations

The optimisation of the sections with respect to local buckling (adding supplementary stiffeners to the section) arises, in this case, a distortional problem.

Early work on the distortional buckling mode in edge-stiffened elements and intermediate stiffened elements was performed by Desmond [13], [14]. In these two papers, the distortional buckling mode was called "stiffener buckling mode", since the stiffener was not adequate to prevent its deformation in a plane normal to the element which it supported.

In a more recent research, Dinis et al. [15] studied the elastic and elastic-plastic local-plate and distortional post-buckling behaviour of rack and lipped channel cold-formed steel columns. That the nature of the critical sectional buckling mode of a given thin-walled member depends, basically, on its (i) cross-section geometry (shape and dimensions) and (ii) end support conditions [16], [17].

For experimental testing, the "fully pinned restraint" cannot be fulfilled due to physical limitations (it is very difficult to axially load a column and to allow warping). Even if the end boundary conditions are different for distortional buckling mode, the linear buckling analysis can provide useful information regarding the failure mode of a studied section. Considering the test results, it can be concluded that for RS125x3.2 sections, the dominant failure mode is a symmetric distortional buckling.

For presented study only the RS125x3.2 section was considered since the RS95x2.6 section is not prone to distortional buckling. Using the calibrated numerical model, the influence of end restraints was studied for the two pallet rack upright sections, considering two types of end restraints:

i) pined and warping restrained (WP);
ii) pinned and free warping (WF).

In the first case (WP), for one end, pinned, the displacement was restrained on all three directions together with the rotation about the longitudinal axis of the element. At the other end, where the force was applied, the translations perpendicular to the longitudinal axis were restrained together with the rotation about the longitudinal axis, while the translation along the longitudinal axis was allowed. The load was applied in the centre of gravity at one end, while the other was considered to be restrained to move.

For the second case (WF) in order to allow the warping of the end sections, the translations perpendicular to the longitudinal axis were restrained, while the translation along the profile longitudinal axis was allowed. To prevent the rigid body translation of the profile, the middle section translation along the longitudinal axis was restraint. The load was applied on the sections' midline.

The two types of the restraints used for numerical simulations are presented in Figure 9.

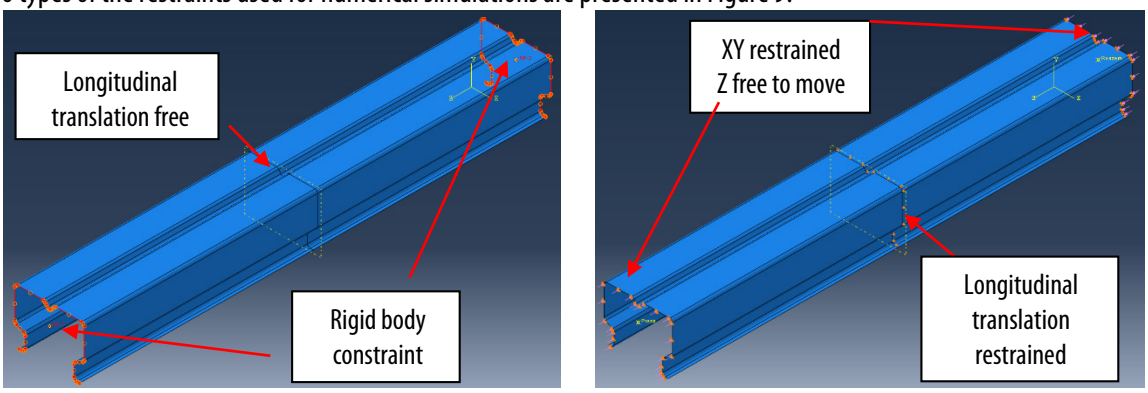

a. Warping prevented ends (WP) b. Free warping ends (WF)

Figure 9. Numerical model restraints

Further, a buckling analysis (warping free - WF and warping prevented - WP) was conducted to evaluate the influence of end restraints. For the analysis, two intervals were considered. The first interval considers the distortional buckling mode as reference (critical buckling length for distortional buckling), while the second interval considers the coupling of the distortional and global flexural buckling.

In order to determine the distortional buckling half-wavelength (critical buckling length for distortional buckling) for the column under study, a LBA was carried using CUFSM software [18]. Further, the coupling length for interactive buckling (i.e. distortional and global flexural buckling about the minor axis) was determined using the ECBL approach [19]. For detailed information see [20], [21].

The analyses were conducted onto two ranges as presented in Table 7:

i) distortional half-wavelength (row "D");
ii) interactive buckling interval (distortional and flexural buckling) (row "I").

Table 7. Length ranges for distortional (D) and Interactive buckling analyses (I)

	Unperforated Sections	Perforated Sections
D	400 ... 800mm	400 ... 800mm
I	2050 ... 2550mm	2350 ... 2750mm

In Figure 10 is presented the buckling mode for a 550mm RS125 profile without perforations considering WP (warping prevented) and WF (warping free) ends.

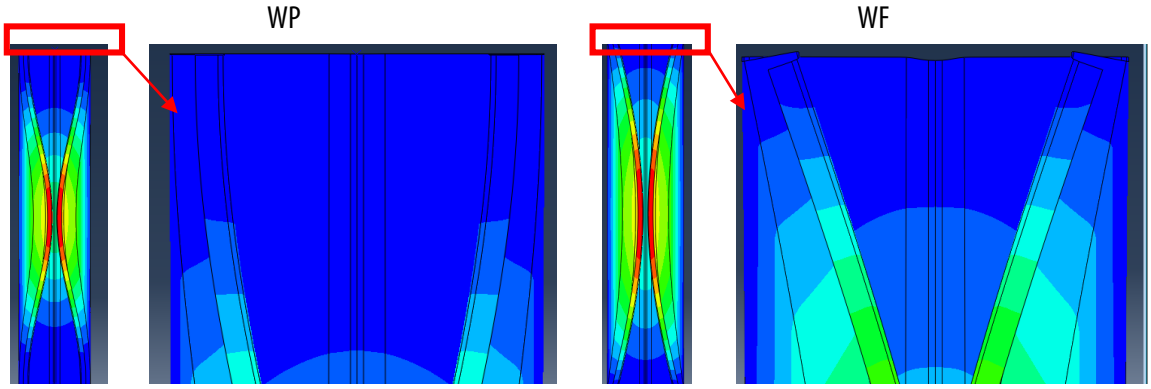

Figure 10. Buckling mode for 550mm RS125x3.2 section without perforations

There is a significant difference between the distortional capacity of pinned end and a fixed end member. The capacity difference is depicted in Figure 11 for RS125x3.2 section without perforations. The analysis was conducted using GBTool [22]. It allows to compute the buckling signature curve for a specific buckling mode (local, distortional or global – flexural or torsional etc., or coupling between them) at any given length.

Analysing Figure 11, it can be observed that when determining the coupling length for interactive buckling, there is no influence of boundary conditions (WF or WP). This can be explained by the fact that for elements longer than three times the distortional buckling critical length (computed with warping free ends) the middle wave can be considered to be free to warp, hence the effect of end restrained is cancelled.

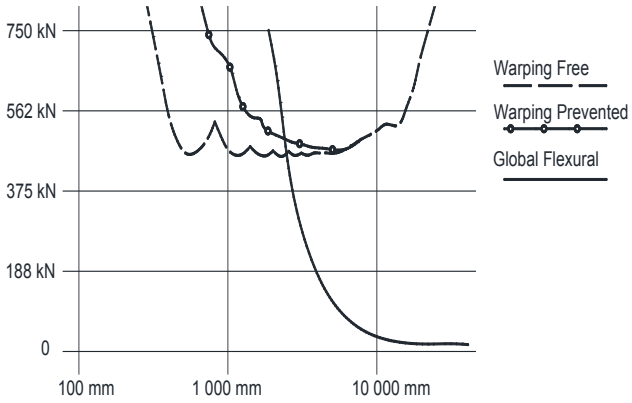

Figure 11. Distortional buckling signature curve for RS125x3.2

3.3. Numerical simulations results

The buckling loads for unperforated (see Figure 12a) and perforated (see Figure 12b) RS125x3.2 section, considering the warping free case (WF) and warping prevented one (WP) are presented.

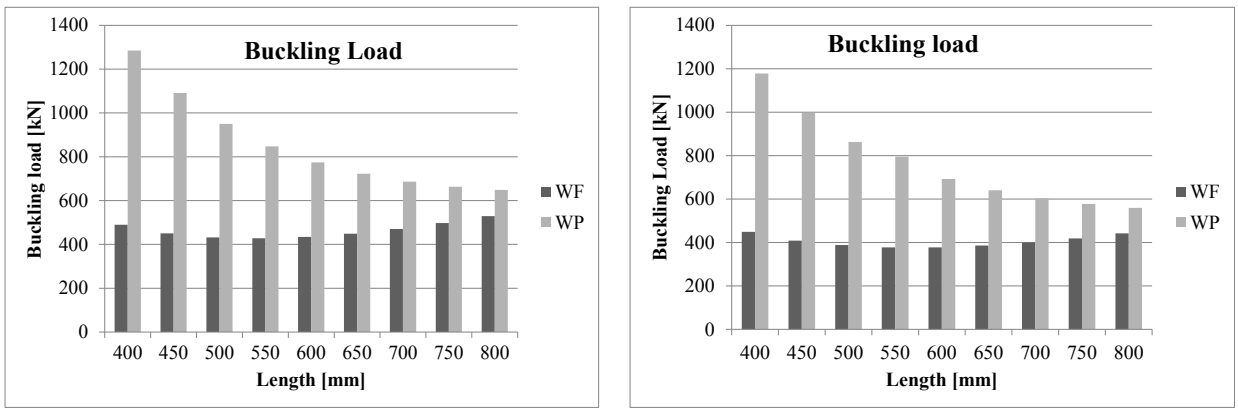

a. Buckling load – RS125 without perforations

b. Buckling load – RS125 with perforations

Figure 12. Buckling loads for RS125x3.2 short columns

Following the analysis of results for buckling loads and ultimate loads for short columns (half-wave length for distortional buckling), using the ECBL approach [19], the interactive buckling length was computed [20], [21]. Based on the interactive buckling length an interactive buckling rage was defined (approximately ±10% around the coupling length).

The buckling loads for columns in interactive buckling (considering only the distortional buckling mode) are presented in Figure 13a for the section without perforations and in Figure 13b for the section with perforations [23].
The buckling loads for columns in interactive buckling (considering only the global buckling mode) are presented in Figure 14a for the section without perforations and in Figure 13b for the section with perforations.

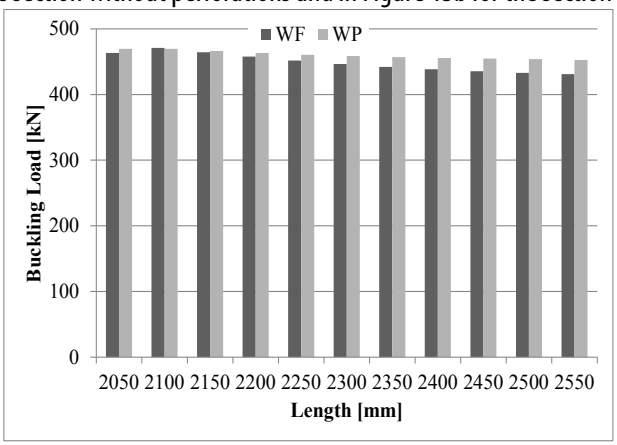

a. RS125x3.2 without perforations

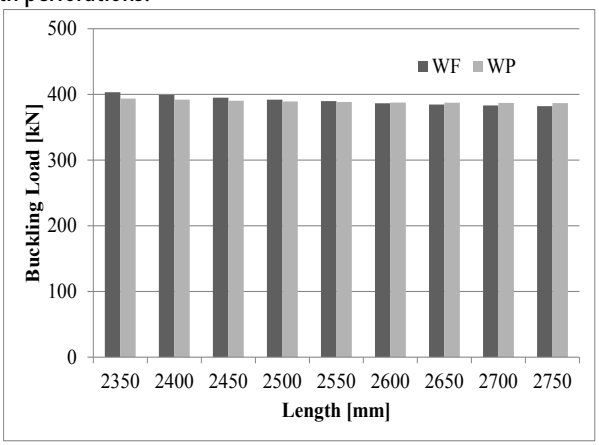

b. RS125x3.2 with perforations

Figure 13. Buckling loads for RS125x3.2 long columns – distortional failure mode

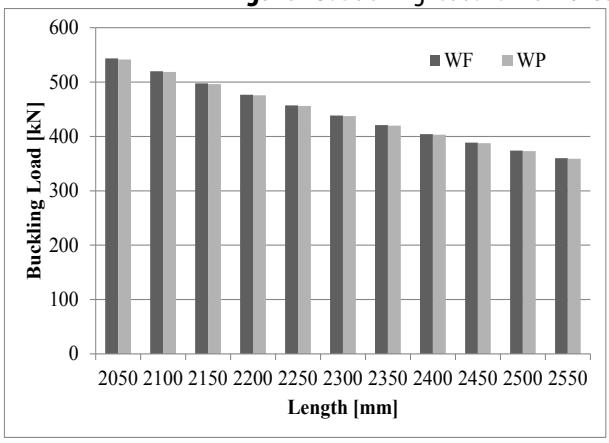

a. RS125x3.2 without perforations

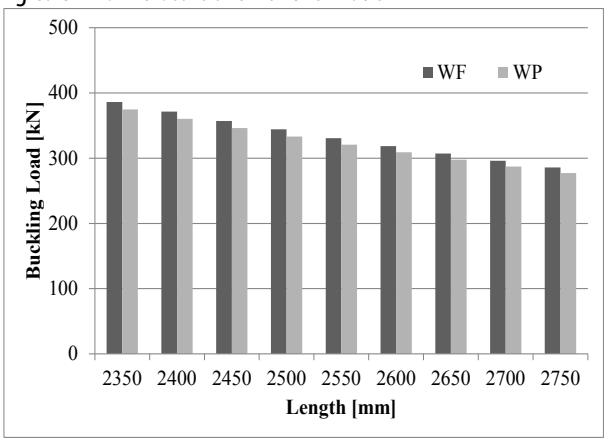

b. RS125x3.2 with perforations

Figure 14. Buckling loads for RS125x3.2 long columns – global failure mode

4. CONCLUDING REMARKS

Present paper presents the main outcome of an extend experimental and numerical study carried out within the CEMSIG Research Centre (http://cemsig.ct.upt.ro), dep. of Steel Structures and Structural mechanics, POLITEHNICA University of Timisoara.
In accordance with EN15512:2009 [1] design code, two axial compression tests are carried out in order to determine the uprights' capacity i.e. stub column tests to determine the influence of local buckling and perforations and an upright column test to determine the influence of distortional buckling. Considering the experimental results, the upright tests prescribed by the code may correspond to an interactive buckling rather than distortional buckling.
The calibrated numerical models, using the measured material properties and imperfections were validated for all experimentally tested specimens. It can be observed that the calibrated numerical model is able to reproduce the experimental tests with high accuracy, limiting the number of necessary experimental testing.
The influence of warping end constraints it is of paramount importance when determining the sectional capacity (see Figure 12), but its effect fades when dealing with long elements (see Figure 13 and Figure 14). Furthermore, it can be said that, if the element has the length higher than three times the critical length associated with distortional buckling, the mid-half-wave can be considered as being pinned.

Acknowledgement

This work was partially supported by the strategic grant POSDRU/159/1.5/S/137070 (2014) of the Ministry of National Education, Romania, co-financed by the European Social Fund – Investing in People, within the Sectorial Operational Programme Human Resources Development 2007-2013.

References

[1] EN15512:2009. Steel static storage systems - Adjustable pallet racking systems - Principles for structural design, CEN, Brussels, 2009.

[2] EN1993-1-3. Eurocode 3 – Part 1-3: "Supplementary rules for cold-formed thin gauge members and sheeting". Published by European Committee for Standardization, Brussels, 2006
[3] Thomasson P. Thin-walled C-shaped panels in axial compression. Swedish Council for Building Research. D1:1978, Stockholm, Sweden, 1978.
[4] Hancock GJ. Distortional buckling of steel storage rack columns. Journal of Structural Engineering, ASCE, 111(12), 2770-2783, 1985.
[5] Lau SCW. Distortional buckling of thin-walled columns. PhD Thesis, University of Sydney, Sydney, Australia, 1988.
[6] Schafer BW. Local, distortional and Euler buckling of thin-walled columns. Journal of Structural Engineering, ASCE, 128(3), 289-299, 2002.
[7] Schafer BW, Pekoz T. Direct strength prediction of cold-formed steel members using numerical elastic buckling solutions. Proceedings of the Second International Conference on Thin-Walled Structures: Research and Development. Singapore, 137-144, 1998.
[8] Moen CD, Schafer BW. Direct strength design of cold-formed steel members with perforations. Research Report RP09-1, The Johns Hopkins University, USA, 2009.
[9] Crisan A. Buckling strength of cold-formed steel sections applied in pallet rack structures. PhD Thesis, "POLITEHNICA" University of Timisoara, Civil Engineering Faculty, Ed. Politehnica, Seria 5: Inginerie Civila, No. 76, 2011
[10] EN10002-1, "Tensile testing of metallic materials. Method of test at ambient temperature", Published by European Committee for Standardization, Brussels, 2001
[11] Crisan, A., Ungureanu, V. and Dubina, D., 2012a, Behaviour of Cold-formed Steel Perforated Sections in Compression: Part 1 - Experimental investigations, Thin-Walled Structures, Vol.61, pp.86-96.
[12] ABAQUS, Theory manual, Hibbit, Karlson and Sorenson Inc., 2007.
[13] Desmond TP, Pekoz T, Winter G. Edge stiffeners for thin-walled members. Journal of Structural Engineering - ASCE, vol. 107, no. 2, pp. 329-53, 1981a.
[14] Desmond TP, Pekoz T, Winter G. Intermediate stiffeners for thin-walled members. Journal of Structural Engineering - ASCE, vol. 107, no. 4, pp. 627-48, 1981b.
[15] Dinis PB, Camotim D, Silvestre N. FEM-based analysis of the local-plate/distortional mode interaction in cold-formed steel lipped channel columns. Journal of Computers and Structures, vol. 85, no. 19-20, pp. 1461-1474, 2007.
[16] Camotim D, Prola LC. On the Stability of Cold-Formed Steel Structural Elements with Rack Sections. Proceedings 5th International Colloquium on Structural Stability (Brazilian Session), Rio de Janeiro, Brazil, pp. 21-32, 1996.
[17] Prola LC. Local and global stability of cold-formed steel members. Ph.D. Thesis, Technical University of Lisbon (in Portuguese), 2001.
[18] Li Z, Schafer BW. Buckling analysis of cold-formed steel members with general boundary conditions using CUFSM: conventional and constrained finite strip methods. Proceedings of the 20th International Specialty Conference on Cold-Formed Steel Structures, St. Louis, MO. November, 2010.
[19] Dubina D. The ECBL approach for interactive buckling of thin-walled steel members. Steel and Composite Structures, vol. 1, no. 1, pp. 75-96, 2001
[20] Crisan A, Ungureanu V, Dubina D. Behaviour of cold-formed steel perforated sections in compression. Part 1 – Experimental investigations. Thin-Walled Structures, vol. 61, pp. 86-96, 2012a.
[21] Crisan A, Ungureanu V, Dubina D. Behaviour of cold-formed steel perforated sections in compression. Part 2 – Numerical investigations and design considerations. Thin Walled Structures, vol. 61, pp. 97-105, 2012b.
[22] Bebiano R, Pina P, Silvestre N, Camotim D. GBTUL – Buckling and Vibration Analysis of Thin-Walled Members. DECivil/IST, Technical University of Lisbon (http://www.civil.ist.utl.pt/gbt), 2008.
[23] Andrei Crisan, Viorel Ungureanu, Dan Dubina "Influence of end restraints on storage racks uprights axial strength", proceedings of the C60 international conference, p. 103 ISBN 978-973-662-903-7, 2013